The establishment of axial patterning in the maize leaf

Toshi Foster[1,*,†], Angela Hay[2,*], Robyn Johnston[3] and Sarah Hake[4]

[1]The Horticulture and Food Research Institute of New Zealand, Private Bag 11 030, Palmerston North, New Zealand
[2]Department of Plant Sciences, Oxford University, South Parks Road, Oxford, OX1 3RB, UK
[3]Institute of Molecular BioSciences, Massey University, Private Bag 11 222, Palmerston North, New Zealand
[4]Plant Gene Expression Center, 800 Buchanan Street, Albany, CA 94710, USA
*These authors contributed equally to the work
[†]Author for correspondence (e-mail: tfoster@hortresearch.co.nz)

Accepted 11 May 2004

Development 131, 3921-3929
Published by The Company of Biologists 2004
doi:10.1242/dev.01262

Summary

The maize leaf consists of four distinct tissues along its proximodistal axis: sheath, ligule, auricle and blade. *liguleless1* (*lg1*) functions cell autonomously to specify ligule and auricle, and may propagate a signal that correctly positions the blade-sheath boundary. The dominant *Wavy auricle in blade* (*Wab1*) mutation disrupts both the mediolateral and proximodistal axes of the maize leaf. *Wab1* leaf blades are narrow and ectopic auricle and sheath extend into the blade. The recessive *lg1-R* mutation exacerbates the *Wab1* phenotype; in the double mutants, most of the proximal blade is deleted and sheath tissue extends along the residual blade. We show that *lg1* is misexpressed in *Wab1* leaves. Our results suggest that the *Wab1* defect is partially compensated for by *lg1* expression. A mosaic analysis of *Wab1* was conducted in *Lg1*+ and *lg1-R* backgrounds to determine if *Wab1* affects leaf development in a cell-autonomous manner. Normal tissue identity was restored in all *wab1*+/– sectors in a *lg1-R* mutant background, and in three quarters of sectors in a *Lg1*+ background. These results suggest that *lg1* can influence the autonomy of *Wab1*. In both genotypes, leaf-halves with *wab1*+/– sectors were significantly wider than non-sectored leaf-halves, suggesting that *Wab1* acts cell-autonomously to affect lateral growth. The mosaic analysis, *lg1* expression data and comparison of mutant leaf shapes reveal previously unreported functions of *lg1* in both normal leaf development and in the dominant *Wab1* mutant.

Supplemental data available online

Key words: Maize, *liguleless1*, *Wavy auricle in blade1*, Leaf development, Axial patterning, Mosaic analysis, Cell autonomy

Introduction

The diversity of leaf shape in the plant kingdom reflects subtle differences in morphogenetic events that are similar for all plants. Leaves are initiated from groups of cells on the flanks of the shoot apical meristem (SAM) and acquire their characteristic form shortly after emergence. At maturity, leaves are asymmetric about one or more axes: proximodistal (base to tip), adaxial-abaxial (upper to lower surface) and mediolateral (midvein to margins). The asymmetric distribution of cell types, vasculature, air spaces, epidermal hairs and cuticular waxes allow each part of the leaf to perform a specialised function. Relatively little is known about the mechanisms that pattern each axis of the leaf.

Clonal analysis of leaf development indicates that the number of leaf founder cells ranges from about 30 in *Arabidopsis* to approximately 250 in tobacco and maize (Poethig, 1984; Furner and Pumfrey, 1992; Irish and Sussex, 1992; Poethig and Szymkowiak, 1995). In most dicots, the leaf founder cells occupy only a portion of the radial dimension of the SAM, whereas in maize, a complete ring of leaf founder cells surrounds the SAM (Steffensen, 1968). Most dicot leaves first appear as peg-like outgrowths that subsequently grow in the lateral dimension to form a flattened blade. Substantial evidence suggests that the juxtaposition of adaxial and abaxial cell types stimulates lamina outgrowth in dicot leaves (Waites and Hudson, 1995; McConnell and Barton, 1998; Bowman, 2000; Kerstetter et al., 2001). In contrast, the maize leaf has a lamina from inception, and furthermore, a number of mutations affect or even delete specific lateral domains without affecting abaxial-adaxial asymmetry (Scanlon et al., 1996; Fowler and Freeling, 1996; Foster et al., 1999). These findings suggest that fundamentally different sequences of pattern formation occur in monocot and dicot leaves.

As the emerging leaf primordium grows away from the SAM, a new proximodistal axis of growth is established, and cells differentiate according to positional cues within the developing organ (McConnell et al., 2001; Matsumoto and Okada, 2003). In maize leaves, four distinct tissues develop along the proximodistal axis. The proximal sheath and distal blade are separated by a fringe of ligule tissue and two wedges of auricle tissue (Fig. 1E). The recessive *liguleless1* (*lg1*) and *lg2* mutations remove ligule and auricle, but do not affect the specification of blade and sheath (Emerson, 1912; Brink, 1933). *lg1* is expressed in leaf primordia in the zone of the developing ligule and encodes a SQUAMOSA PROMOTER-BINDING protein (Moreno et al., 1997). Mosaic analysis has shown that *lg1* functions cell autonomously to specify ligule and auricle (Becraft et al., 1990). *lg1* has also been implicated

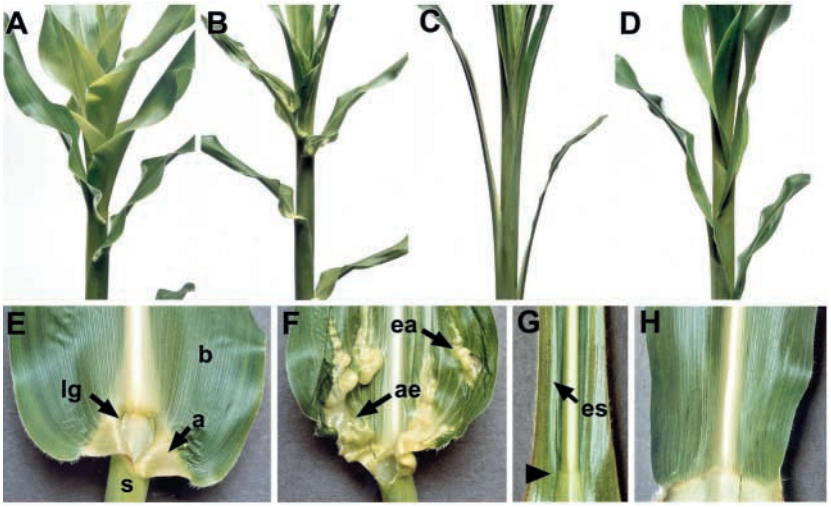

Fig. 1. Leaf and whole plant phenotypes 8 weeks after planting. (A) Wild-type, (B) *Wab1*, (C) *lg1-R;Wab1* and (D) *lg1-R* plants. (E-H) Adaxial view of blade-sheath boundary of (E) wild-type, (F) *Wab1*, (G) *lg1-R;Wab1*, and (H) *lg1-R* leaves. a, auricle; b, blade; ae, auricle extension; ea, ectopic auricle; es, ectopic sheath; lg, ligule; s, sheath. Arrowhead in G indicate presumptive blade-sheath boundary in *lg1-R;Wab1* leaf.

in the propagation of a signal to initiate ligule and auricle (Becraft and Freeling, 1991). *lg2*, which encodes a bZIP transcription factor, is expressed ubiquitously throughout the leaf primordia and functions non-cell autonomously as shown by mosaic analysis (Harper and Freeling, 1996; Walsh et al., 1998). Based on double mutant analysis, it has been suggested that *lg1* and *lg2* function in the same pathway (Harper and Freeling, 1996).

Wab1 is a recently described dominant mutation that disrupts both mediolateral and proximodistal patterning of the maize leaf resulting in narrow leaves and inappropriate cell differentiation (Hay and Hake, 2004). We constructed double mutants between *Wab1* and *lg1-R* and *lg2-R* to analyse the effect that loss of auricle tissue would have on the *Wab1* phenotype. Double mutant leaves are very narrow and sheath tissue extends along the residual blade. Genetic mosaics of *wab1+/–* were created in *Wab1* and *lg1-R;Wab1* mutants to determine if *Wab1* disrupts leaf patterning in a cell-autonomous manner. The mosaic analysis indicates that *Wab1* generally acts autonomously but may be influenced by *lg1*. Our data reveal previously unreported roles for *lg1* in leaf development and support a model in which signalling via *lg1* is required to correctly position the blade-sheath boundary (Becraft and Freeling, 1991).

Materials and methods

Genetic stocks and irradiation conditions

F_3 families segregating 1:1 for *lg1-R: lg1-R;Wab1/wab1+* and 1:1 for *lg2-R: lg2-R; Wab1/wab1+* were used for phenotypic analyses. *lg1-R* introgressed at least four times into the W23 genetic background was used for *lg1-R* leaf measurements. See supplemental data (http://dev.biologists.org/supplemental/) for more details. For the mosaic analysis of *Wab1*, heterozygous *Wab1-R* plants were crossed to Maize Genetic Coop stocks heterozygous for *white seedling3* (*w3*). For the mosaic analysis of *lg1-R;Wab1*, *lg1-R/lg1-R;Wab1/+* plants were crossed to *lg1-R/lg1-R; v4/v4, w3/+* stocks from the Maize Genetic Coop. In accordance with maize nomenclature, we refer to the wild-type alleles as *Lg1+* and *wab1+*, the mutant alleles as *lg1-R* (reference allele) and *Wab1* (*Wab1-R*), and the wild-type genes as *lg1* and *wab1*. See Fig. S1 (http://dev.biologists.org/supplemental/) for a schematic of the genetic material used in the mosaic analysis.

Seeds were allowed to imbibe for 48 hours at 25°C then irradiated with approximately 1,500 rads. The radiation was from a 6 MV photon (X-ray) beam generated by a linear accelerator at the Palmerston North Hospital Radiotherapy Unit, Palmerston North, New Zealand. Irradiated seeds were hand planted into soil at the Institute of Developmental Phenomenology, Raumai, New Zealand.

Sector analysis

Plants were grown to maturity and screened for albino (*w3/–*), and yellow (*v4/–*) sectors throughout development. Out of 1681 irradiated seeds, 93 *w3 wab1+/–* sectored leaves were identified in 42 *Wab1/wab1+* plants and 51 sectored leaves were identified in 32 *wab1+/wab1+* control plants. In the second experiment, 4,608 seeds were irradiated; 115 *w3 wab1+/–* sectors and 65 *v4 wab1+/–* sectors were identified in 81 *lg1-R/lg1-R*; *Wab1/wab1+* plants. In 46 *lg1-R/lg1-R*; *wab1+/wab1+* control plants, 90 *w3 wab1+/–* and 50 *v4 wab1+/–* sectors were analysed. All sectored leaves were harvested at maturity and photographed and/or photocopied. Leaf number, sector width and the lateral position of the sector within the blade and sheath were recorded. See supplemental material (http://dev.biologists.org/supplemental/) for details of data analysis.

Transverse hand sections of freshly harvested sectored leaves were examined by epifluorescence microscopy using a Leica (MZFLIII) stereomicroscope equipped with a 395-440 nm excitation filter and a 470 nm observation filter. All sections were photographed using a DC200 digital camera (Wetzlar, Germany). Under these conditions, normal chloroplasts fluoresce bright red and cell walls appear blue-green. No chlorophyll autofluorescence is detected in *w3/–* cells. The presence or absence of chlorophyll in epidermal layers was scored by inspecting guard cells, the only chloroplast-containing cell-type in the epidermis. Sectors of *v4/–* appear yellow because of a delay in the accumulation of chlorophyll, but eventually become green. Boundaries of *v4* sectors were marked with a pen.

Scanning electron and light microscopy

Mature leaf tissue was fixed in 3% glutaraldehyde and 2% paraformaldehyde in 0.1 M phosphate buffer. Prior to fixation, a small notch was made at the sector boundary (SEM samples only). Samples for SEM were dehydrated in acetone, critical-point dried in liquid CO_2 and sputter coated with 25 nm gold using a Polaron E 5400 sputter coater (SCD-050; Bal-Tec, Balzers, Liechtenstein). Specimens were examined on a Cambridge 250 Mark III scanning electron microscope (Cambridge Instruments, Cambridge, UK) operated at 20 kV, and images were captured on 35 mm film. Samples for light microscopy were infiltrated and embedded in Procure 812 (ProSciTech, Kelso, Australia). Sections (1 μm) were cut, heat mounted, stained with 0.05

(w/v) Toluidine Blue and photographed with an Axioplan microscope equipped with an Axiophot camera (Zeiss, Jena, Germany).

lg1 and *lg2* gene expression

Leaf primordia (P9-10) were removed from the shoot, the ligule region dissected and immediately placed in liquid nitrogen. Leaf primordia (P6-8) were removed, dissected 5 mm above their base for a pre-ligule tissue sample and a further 5 mm above this for a blade tissue sample and immediately placed in liquid nitrogen. The remaining five plastochrons and SAM were used as a SAM sample. Each RNA sample consisted of a pool of ten seedlings. Tissue dissection, RNA isolation and cDNA synthesis were each performed twice independently, in each case giving identical results. Gene-specific PCR primers were as described for *lg1* (Moreno et al., 1997) and *lg2* (Walsh et al., 1998). 20 PCR cycles were performed and amplified products were detected by Southern hybridization with gene-specific probes.

Results

lg1-R and *lg2-R* enhance the *Wab1* mutant phenotype

Four distinct tissue types demarcate the proximodistal axis of a wild-type maize leaf, the proximal sheath and distal blade are separated by ligule and auricle tissues (Fig. 1A,E). The ligule is an epidermally derived fringe, and the auricles are thickened wedges of tissue that act as a hinge between blade and sheath (Sharman, 1941; Becraft et al., 1990). Each of these tissue types has characteristic epidermal features and histological organisation, which have been well characterised by scanning electron and light microscopy (Fig. 2A-G) (Sharman, 1942; Esau, 1977; Russell and Evert, 1985; Langdale et al., 1989; Sylvester et al., 1990).

The *Wab1* mutation disrupts normal patterning of the leaf and results in patches of ectopic auricle, sheath and ligule in the leaf blade (Fig. 1F) (Hay and Hake, 2004). Often a localised increase in blade width occurs immediately distal to patches of ectopic auricle. In addition, the normally placed auricle is more extensive, spreading distally into the leaf blade. Long strips of thickened auricle tissue and the reduced lamina width give *Wab1* plants an unusual appearance; narrow, rigid leaves extend from the main axis at a more obtuse angle than wild-type leaves (Fig. 1B). Examination of histological and epidermal features reveals that the *Wab1* blade contains cells with auricle and sheath identity (Fig. 2I,J,L). In both ectopic sheath and auricle tissue, intermediate veins fuse into lateral veins, and normal bundle sheath anatomy is absent or incomplete (arrowheads in Fig. 2I,J).

We constructed double mutants between *Wab1* and *lg1-R* and *lg2-R* to analyse the effect that loss of auricle tissue would have on the *Wab1* phenotype. The recessive *lg1* and *lg2* mutations remove ligule and auricle, giving the mutant leaves a more upright appearance (Fig. 1D) (Harper and Freeling, 1996). Despite the lack of ligule and auricle, *lg1-R* and *lg2-R* leaves have a distinct boundary between blade and sheath (Fig. 1H). *lg1-R* affects all but the uppermost leaves, whereas *lg2-R* only affects juvenile leaves (Harper and Freeling, 1996). *lg1-R;Wab1* double mutants exhibit a striking, narrow leaf phenotype (Fig. 1C,G). Both the normal and ectopic auricle tissue is absent in the double mutant, most of the proximal blade deleted and sheath-like tissue extends along the margins

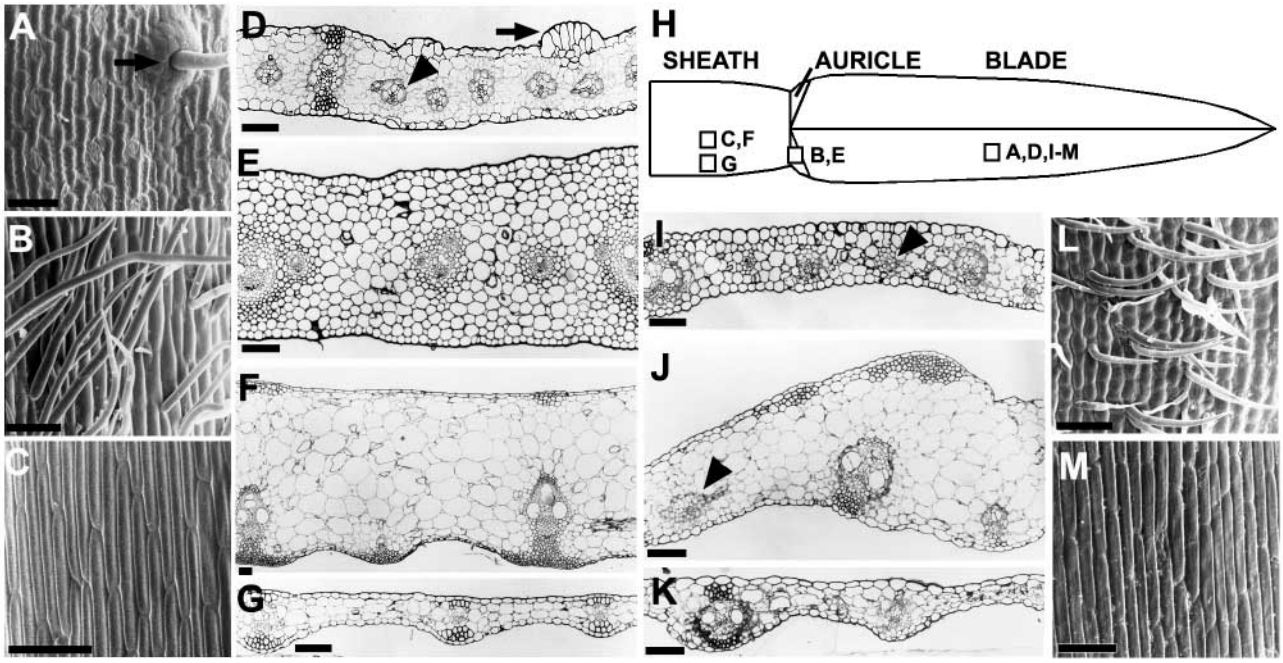

Fig. 2. Scanning electron and light micrographs illustrating epidermal and histological features of wild-type and mutant leaves. (A-C) SEM of adaxial surface of wild-type (A) blade, (B) auricle and (C) sheath. (D-G) Transverse section through wild-type (D) blade, (E) auricle, (F) internal sheath and (G) marginal sheath tissue. (H) Cartoon depicting regions where tissue was sampled. (I-K) Transverse sections through (I) ectopic auricle in *Wab1* blade, (J) ectopic sheath in *Wab1* blade and (K) ectopic sheath in *lg1-R;Wab1* blade. (L-M) SEM of adaxial surface of (L) *Wab1* ectopic auricle and (M) *lg1-R;Wab1* ectopic sheath. All sections are oriented with the adaxial surface upwards. Arrows in A and D indicate multicellular base of macrohair. Normal bundle-sheath anatomy indicated by arrowhead in D, abnormal bundle-sheath anatomy indicated by arrowheads in I and J. Scale bars: 100 μm.

of the residual blade. *lg2-R;Wab1* and *lg1-R;lg2-R;Wab1* mutants are similarly affected (data not shown).

The ectopic tissue in *lg1-R;Wab1* leaf blades has histological and epidermal features of sheath. The adaxial surface is hairless and cells are long with smooth cell wall junctions (Fig. 2M), but the abaxial surface is covered with hairs specific to abaxial sheath tissue (not shown). *lg1-R;Wab1* sheath-like tissue is very thin in the transverse dimension (Fig. 2K) and the intervascular spacing and prominent transverse veins resemble those found in marginal sheath tissue (Fig. 2G). In distal positions and near the midrib, *lg1-R;Wab1* leaves have normal blade tissue (not shown). Sheath tissue identity is not affected by the *lg1*, *lg2* or *Wab1* mutations.

lg1-R leaf shape

Although the *lg1-R* ligule defect has been well described by others, the altered shape of *lg1-R* leaves has not been reported. We found that *lg1-R* leaves are significantly narrower at the blade-sheath boundary than those of non-mutant (*Lg1+*/*lg1-R*) siblings (Table S1, http://dev.biologists.org/supplemental/). The mean width of the ninth leaf counting down from the tassel was 76 mm for *lg1-R* plants, whereas, the mean width was 102 mm for non-mutant siblings. A similar trend was seen for the tenth and eleventh leaves down from the tassel. We also noted that while the overall lengths of *lg1-R* and *Lg1+*/*lg1-R* leaves are the same, *lg1-R* blades are shorter and *lg1-R* sheaths are longer than those of non-mutant siblings (Table S1). This finding indicates that the blade-sheath boundary is established in a more distal position in the *lg1-R* mutant.

We compared the width of *w3*-marked clonal sectors in wild-type (*Lg1+*/*Lg1+*) and *lg1-R* plants. Sectors were measured at the base of the blade. Only sectors in adult leaves were included in this analysis to minimise variation in leaf size (see Supplemental data, http://dev.biologists.org/supplemental/). Sectors near the midrib had similar median widths in wild-type and *lg1-R* blades. However, sectors in lateral and marginal regions were significantly narrower in *lg1-R* mutants than in wild-type leaves (Table S2, http://dev.biologists.org/supplemental/). These data indicate that the *lg1-R* lateral growth defect is localised to lateral and marginal domains of the blade.

lg1 is misexpressed early in development of *Wab1* leaves

The dramatic effect of *lg* mutations on the *Wab1* phenotype suggests that the presence of *lg1* and *lg2* partially compensates for the defects in leaf width and tissue identity in *Wab1* mutants. We carried out RT-PCR to see if *lg1* or *lg2* were expressed differently in *Wab1* mutants. Previous efforts to detect *lg1* or *lg2* by in situ hybridisation have not been successful (Moreno et al., 1997) (Walsh and Freeling, personal communication). *lg1* transcript is absent from wild-type tissue samples containing the SAM and P1-5 primordia, but expression is detected in equivalent *Wab1* tissue at 20 PCR cycles (Fig. 3). This early expression in *Wab1* was confirmed using a dilution of cDNA in the PCR reaction. Transcript was never detected in equivalent wild-type tissue at 40 PCR cycles (data not shown). *lg1* expression was detected in both wild-type and *Wab1* leaf primordia in the preligule band region of P6-8 and the ligule ridge region of P9-10 leaves (Fig. 3). Transcript was absent from the blade region of wild-type P6-8 leaves at 20 PCR cycles. Expression of *lg1* was reproducibly detected in the blade region of *Wab1* P6-8 primordia at 20 PCR cycles and confirmed using a dilution of cDNA in the PCR reaction. This result indicates that the expression domain of *lg1* extends distally in *Wab1* leaf primordia, consistent with the distal extension of auricle tissue in mature *Wab1* leaves.

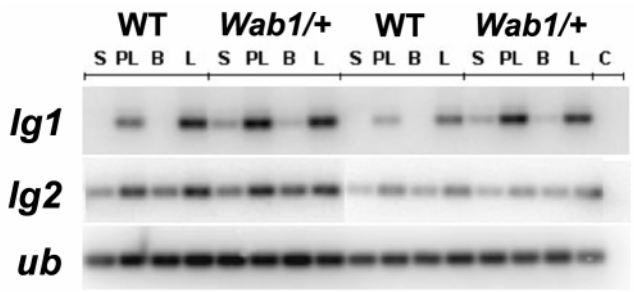

Fig. 3. *lg1* and *lg2* expression in *Wab1* leaves. RT-PCR gel blot analysis of *lg1* and *lg2* expression in 4-week-old seedlings of wild-type and *Wab1*/+ at the following stages of leaf development: SAM including P1-5 (S), P6-8 pre-ligule region (PL), P6-8 blade (B), P9-10 ligule region (L). Lanes 9-16 are as for lanes 1-8 using a four-fold dilution of cDNA. Control with no cDNA included in PCR (C). Control amplification of *ubiquitin* (*ub*) indicates equal amounts of cDNA present in each sample.

No significant difference in *lg2* mRNA expression could be detected in *Wab1* compared with wild-type plants in any of the tissue samples analysed (Fig. 3).

Mosaic analysis of *Wab1*

Sectors of tissue lacking the dominant *Wab1* allele (*wab1+*/–) were created in both *Wab1* and *lg1-R;Wab1* mutants to determine if *Wab1* disrupts leaf patterning in a cell-autonomous manner (Fig. S1, http://dev.biologists.org/supplemental/). Stocks carrying *Wab1* in repulsion to *white seedling3* (*w3*) were X-irradiated to induce random chromosome breaks. Radiation-induced breaks proximal to *W3* resulted in albino, non-*Wab1* (*w3 wab1+*) sectors in otherwise green, *Wab1* or *lg1-R;Wab1* plants. In *lg1-R;Wab1* plants, chromosome breaks proximal to *Virescent4* (*V4*) created yellow, *lg1-R* (*v4 wab1+*;*lg1-R*) sectors. The loss of *W3* in normal plants, and either *W3* or *V4* in *lg1-R* plants, provided control sectors that were hemizygous for chromosome 2L.

To ensure that the chromosome arm carrying *Wab1* was lost early in leaf development, only sectors that extended through both the sheath and blade were analysed. Given the variability of the *Wab1* phenotype, only sectors adjacent to tissue displaying a mutant phenotype could be scored. Thus, of 273 total sectors, only 77 were scorable for tissue identity. Sectors adjacent to ectopic auricle and sheath tissue were analysed for phenotypic expression (mutant or wild type) and cell layer composition (green or albino) (Table 1). Because *v4* sectors eventually accumulate normal amounts of chlorophyll, it was difficult to determine the internal layer composition of yellow, *v4* sectors in mature leaves. Thus, only *w3* sectors were scored for albino versus green mesophyll and epidermal layers. We predicted that white or yellow sectors would have normal blade tissue if *Wab1* functions cell autonomously, while the white or yellow sectors would have the same mutant phenotype as the

Table 1. Summary of *wab1*+/– sector phenotypes

Phenotype	Scorable Sectors	All sector types	White L1/ white L2	Green L1/ white L2	White L1/ mixed L2	Green L1/ mixed L2
Wab1						
Ectopic auricle/Auricle extension	31	24 + (77%)	4	17	1	2
		7 W (23%)	1	2	0	4
Wab1						
Ectopic sheath	20	15 + (75%)	0	14	0	1
		5 W (25%)	1	3	0	1
lg1-R;Wab1						
Ectopic sheath	26*	26 + (100%)	10	11	0	1
		0 W (0%)	0	0	0	0

Sectors were scored as '+' if they displayed characteristics of blade tissue, and 'W' if they exhibited auricle or sheath characteristics. Mixed layer sectors that spanned fewer than three veins were included as part of the larger adjacent sector. If adjacent sector types displayed different phenotypes then both were scored. Otherwise, only the sector composition adjacent to green, *Wab1* tissue was scored. *Four yellow (*v4*) sectors were not included in sector subtypes because of difficulties in determining the exact layer composition of *wab1*+ *v4*/– sectors.

adjacent green tissue if *Wab1* acts in a non-autonomous manner.

Ectopic auricle and auricle extension phenotypes in *Wab1* mutants

Sectors were examined using SEM and hand-cut sections to determine the phenotype of *wab1*+/– tissue. In 77% (24/31) of scorable sectors, *wab1*+/– cells exhibited normal blade characteristics whereas adjacent *Wab1* tissue displayed either ectopic auricle or extension of auricle phenotypes (Fig. 4A-E; Table 1). These results indicate that *Wab1* generally acts in a cell-autonomous manner in the lateral dimension to condition ectopic auricle and auricle extension phenotypes.

Fig. 4F is a SEM of the adaxial epidermis of the boxed region shown in Fig. 4C. There is a clear transition from albino *wab1*+/– tissue, which has blade characteristics such as macrohairs (left of arrowhead), to green, hairless *Wab1/wab1*+ tissue with unexpanded dovetailed cells typical of immature auricle (right of arrowhead, Fig. 4F). Green, *Wab1/wab1*+ tissue fluoresces red under UV illumination while albino *wab1*+/– tissue appears blue-green. When sectored tissue is viewed in transverse section, abrupt changes in histology are apparent at the sector boundaries. For example, in Fig. 4G, the

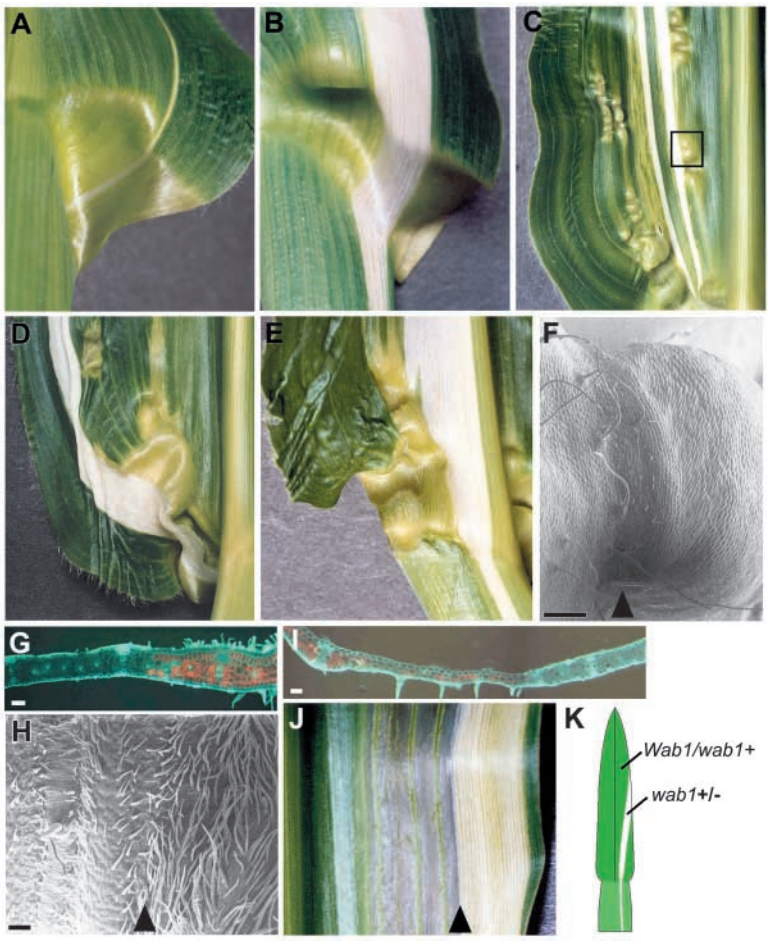

Fig. 4. Sector phenotypes in *Wab1* mutants. (A-E) Abaxial view of *Wab1* leaves with auricle extension and/or ectopic auricle phenotypes with albino sectors exhibiting normal blade characteristics. (F) Scanning electron micrograph of adaxial surface of boxed region in C, illustrating unexpanded, dovetailed auricle-like cells in *Wab1/wab1*+ ectopic auricle tissue (right of arrowhead), and normal blade epidermal characteristics such as macrohairs in the *wab1*+/– sector (left of arrowhead). (G) Fluorescence micrograph of a transverse section through a sector adjacent to auricle extension, illustrating a sharp boundary between green, *Wab1/wab1*+ auricle-like tissue (which fluoresces red), and albino, *wab1*+/– tissue (which appears blue-green). (H) SEM of adaxial surface of sector boundary near that shown in G, with hairy, fully expanded auricle-like cells in the *Wab1/wab1*+ tissue (right of arrowhead) and normal blade cells including prickle hairs and macrohairs in the *wab1*+/– tissue (left of arrowhead). (I) Fluorescence micrograph of a transverse section through the sector shown in J. Green, *Wab1/wab1*+ tissue is very thin with widely spaced veins, a hairless adaxial surface and abaxial hairs characteristic of marginal sheath tissue. Albino *wab1*+/– tissue has the histological organization of normal blade tissue. (J) Abaxial view of sector adjacent to ectopic sheath tissue, arrowhead marks sector boundary. (K) Cartoon depicting an albino non-mutant (*w3 wab1*+/–) sector in a green *Wab1/wab1*+ leaf. Scale bar: 500 μm (F) and 100 μm (G-I).

albino *wab1+/–* tissue has characteristics of blade tissue, whereas the adjacent *Wab1/wab1+* tissue is thicker and auricle-like. The SEM in Fig. 4H shows the same sector boundary, with albino tissue to the left of the arrowhead and green tissue to the right. The green *Wab1/wab1+* tissue has larger mesophyll cells and is densely covered by long hairs without multicellular bases, these cells are characteristics of mature auricle tissue. The albino *wab1+/–* tissue has prickle hairs, macrohairs and cell types typical of blade tissue.

Of the seven sectors that displayed auricle characteristics through all or part of the sector, six had one or more inner layers of green, *Wab1* cells (Table 1). These results indicate that *Wab1* generally acts cell autonomously in the lateral dimension, but may act non-cell autonomously between cell layers.

An interesting pattern was observed in *Wab1* plants with mild auricle extension phenotypes. In most cases, sectors in these plants had an auricle extension to the midrib side of the sector, but recovered normal tissue identity both within the sector and on the marginal side of the sector (e.g. Fig. 4A,B). In plants exhibiting more severe phenotypes such as ectopic auricle and sheath, sectors with normal tissue identity were flanked by mutant tissue on both sides. These results suggest that normal (*wab1+*) cells may have a directional effect on adjacent *Wab1* cells. There was no obvious relationship between recovery of tissue identity and sector size.

Ectopic sheath in *Wab1* and *lg1-R;Wab1* mutants

In *Wab1* mutants, 75% (15/20) of the sectors adjacent to ectopic sheath exhibited normal blade characteristics. These results also indicate that *Wab1* generally disrupts tissue patterning in a cell-autonomous manner (Table 1). Fig. 4J shows an albino sector adjacent to a region of ectopic marginal sheath tissue, and Fig. 4I is a transverse section through this sector boundary. The green, *Wab1/wab1+* mutant tissue has characteristics of marginal sheath tissue; it is thin, has widely spaced veins, the adaxial surface is hairless, and the abaxial surface has long hairs without multicellular bases (Fig. 4I). In contrast, the adjacent albino *wab1+/–* tissue exhibits histological organisation and epidermal features specific to normal blade tissue (Fig. 2D).

In *lg1-R;Wab1* double mutants, all (26/26) scorable *wab1+/–* sectors exhibited normal blade characteristics, indicating that *Wab1* acts completely autonomously in the absence of *Lg1+* (Table 1). The widest sectors were located at the margin, and restored the leaf half to a more normal shape and width (Fig. 5A,B). Fig. 5A shows a yellow *wab1+ v4/–* sector that occurred at the margin. The yellow blade tissue has almost doubled the width of the leaf base. The sector shown in Fig. 5C was sectioned and examined by SEM (Fig. 5E,D). In transverse section, there is a sharp boundary between albino *wab1+/–* blade tissue and green *Wab1/wab1+* tissue with veins appressed against the abaxial surface, typical of sheath (Fig. 5E). The SEM shows crenulated blade cells to the left of the sector boundary (arrowhead), and smooth-walled, elongated sheath-like cells to the right (Fig. 5D). Fig. 5F is a transverse section through another sector boundary, illustrating the abrupt transition between albino blade tissue and green tissue with long abaxial hairs and other characteristics typical of marginal sheath.

In summary, mixed layer sectors behaved differently in *Wab1* and *lg1-R;Wab1* plants. In *Wab1* plants, some mixed layer sectors exhibited the *Wab1* phenotype, whereas none of the mixed layer sectors in *lg1-R;Wab1* plants exhibited the *Wab1* phenotype. Thus, *Wab1* may act non-autonomously between layers or laterally, but only in a *Lg1+* background.

Effect of *Wab1* sectors on leaf width

The leaf blades of *Wab1* and especially *lg1-R;Wab1* mutants are significantly narrower than those of non-mutant siblings. To investigate the effect of *wab1+/–* sectors on *Wab1* and *lg1-R;Wab1* leaf width, the width of sectored and non-sectored halves of each leaf were measured and compared (see Supplemental data, http://dev.biologists.org/supplemental/). In both *Wab1* and *lg1-R;Wab1* plants, there is a small but significant increase in the median width of the sectored half of the blade relative to the non-sectored half (Table 2, Table S3). Measurements made at the sheath midpoint show no significant difference in width between leaf-halves, indicating that the *Wab1* mutation specifically disrupts lateral growth of blade tissue (Table S3). No difference between the widths of sectored and non-sectored leaf-halves is found in wild-type and *lg1* control plants.

Analysis of the data suggested a relationship between sector position and leaf width. In both *Wab1* and *lg1-R;Wab1* plants, sectors near the midrib were not associated with a significant difference in leaf-half width (Table 2A), whereas leaf-halves with sectors in lateral and marginal positions were significantly wider than non-sectored leaf halves.

Many of the widest sectors in *lg1-R;Wab1* plants were yellow, *v4* sectors. To test if there was a difference in behaviour

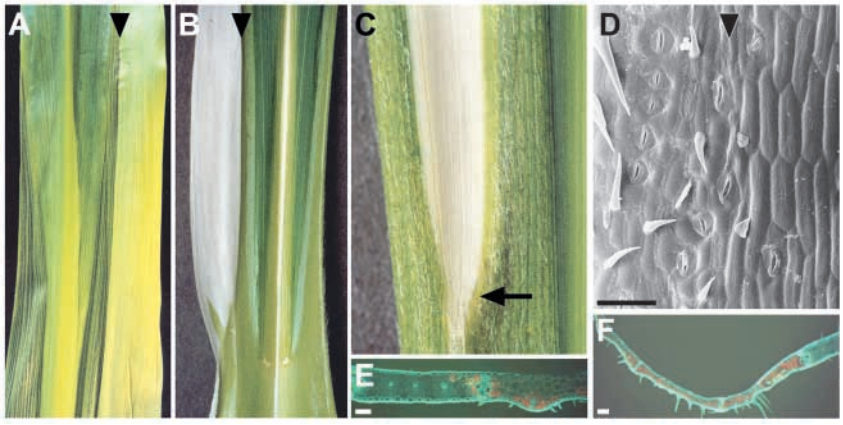

Fig. 5. Sector phenotypes in *lg1-R;Wab1* mutants. (A) Abaxial view of yellow *v4, wab1+/–* sector, and (B) adaxial and (C) abaxial view of white, *w3 wab1+/–* sectors adjacent to ectopic sheath tissue. Arrowheads in A and B mark sector borders. (E) Fluorescence micrograph of a transverse section through the inner sector boundary of leaf shown in C. Green *lg1-R;Wab1* tissue has the histological organisation of sheath, and albino *wab1+/–* tissue that of the blade. (D) SEM of adaxial surface of sector boundary shown in C and D, illustrating the sharp boundary between epidermal cell types in *lg1-R;Wab1/wab1+* tissue (right of arrowhead) and *lg1-R;wab1+/–* tissue (left of arrowhead). (F) Fluorescence micrograph of a transverse section through another sector adjacent to marginal sheath-like tissue. The adaxial surface of green sheath-like tissue in D and F is hairless, whereas the albino tissue has hairs specific to blade. Scale bar: 100 μm (D-F).

Table 2. Median differences in sectored and non-sectored leaf-half widths, and effect of sector position

Genotype	Lateral position of sector	*n*	Median difference (mm)	Significantly different from 0?	*P* value
A					
Wild-type	0.0-1.0	50	0.0	No	1.000
Wab1	0.0-1.0	83	1.0	Yes	0.004
	0.0-0.29	19	0.0	No	1.000
	0.3-1.0	64	1.0	Yes	0.001
lg1-R	0.0-1.0	140	0.0	No	0.440
lg1-R;Wab1	0.0-1.0	180	1.0	Yes	0.000
	0.0-0.29	64	0.0	No	0.390
	0.3-1.0	116	2.0	Yes	0.000
B					
lg1-R;w3	0.3-1.0	44	0.0	No	1.000
lg1-R;v4	0.3-1.0	18	–0.5	No	0.424
lg1-R;Wab1,w3	0.3-1.0	77	1.5	Yes	0.000
lg1-R;Wab1,v4	0.3-1.0	39	3.5	Yes	0.000

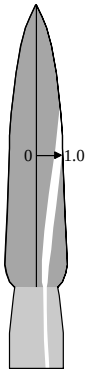

The sectored and non-sectored sides of each leaf were measured from midrib to margin at the blade midpoint. The width of the non-sectored leaf-half was subtracted from that of the sectored half to give an absolute difference in leaf-half width. Differences in leaf-half widths were analysed using a non-parametric 1-sign test to determine if the median values were significantly different from 0 at the 0.05 confidence level (see Supplemental data, http://dev.biologists.org.supplemental/). (A) The relative lateral position of each sector is represented as the distance from the midrib to the closest sector border, divided by the width of the entire leaf-half. Values range from 0 for sectors at the midrib to near 1.0 for sectors at the margin. (B) Median differences were calculated separately for white (*w3*) and yellow (*v4*) sectors in *lg1-R* and *lg1-R;Wab1* leaves.

between *v4* and *w3* sectors, the median difference in leaf-half widths was evaluated separately for yellow and white sectors in *lg1-R;Wab1* and *lg1-R* plants. Sectors near the midrib were not included in this analysis as we had previously determined that they have no significant effect on leaf width. Surprisingly, yellow sectors had a significantly greater effect on leaf width than the white sectors (Table 2B). No difference was detected between yellow and white sectors in *lg1-R* controls, indicating that this effect is not inherent to *v4* sectors, but only occurs in a *Wab1* background.

Discussion

In the maize leaf, ligule and auricle form at the boundary between the blade and sheath. *lg1* has been implicated in the propagation of a signal that correctly positions this boundary, and is necessary for the development of ligule and auricle tissues. The dominant *Wab1* mutation affects mediolateral and proximodistal patterning, resulting in narrow leaves and inappropriate cell differentiation. The recessive *lg1* mutation exacerbates the *Wab1* phenotype. *lg1* expression is activated precociously in *Wab1* leaves and may counteract some effects of the *Wab1* mutation. We conducted a mosaic analysis of *Wab1* in *Lg1+* and *lg1-R* backgrounds to determine if *Wab1* affects leaf development in a cell-autonomous manner. This analysis shows that *Wab1* generally acts cell autonomously to disrupt proximodistal patterning. Examples of *Wab1* non autonomy were only observed in a *Lg1+* background, supporting a role for *lg1* in signal propagation. The mosaic analysis, *lg1* expression data and comparison of mutant leaf shapes reveal previously unreported functions of *lg1* in both normal leaf development and in the dominant *Wab1* mutant.

Lg1+ influences cell autonomy of the *Wab1* phenotype

In the majority of *Wab1* and in all *lg1-R;Wab1* leaves, scorable *wab1+/–* sectors exhibited characteristics of normal blade tissue, whereas adjacent tissue differentiated inappropriately as sheath or auricle. The sharp boundaries between tissue types were coincident with sector boundaries, indicating that *Wab1* generally acts cell autonomously in the lateral dimension to disrupt normal proximodistal patterning.

Twelve of the 51 scorable sectors showed some aspect of the *Wab1* mutant phenotype and thus are exceptions to the general rule of cell autonomy. Of these 12, two were completely albino and therefore had no layer with *Wab1*. Of the 10 remaining sectors, half carried *Wab1* only in the epidermis, and half carried *Wab1* in the epidermis and/or one mesophyll layer. Thus, *Wab1* may act non-autonomously in the lateral dimension and/or between cell layers to influence cell identity in *wab1+/–* tissue.

In contrast, all sectors in *lg1-R;Wab1* plants had normal cell types. *Wab1* in either the epidermis or a single mesophyll layer did not condition the mutant phenotype (12 of 26 sectors). These results suggest that normal *lg1* function is required for *Wab1* to act non-autonomously.

We also observed a few cases of non autonomy in which the normal blade phenotype (*wab1+*) was seen on the margin side of the sector as well as within the sector (e.g. Fig. 4A,B). The extension of the normal phenotype from the sector into genetically *Wab1* cells was only seen in mildly affected plants. This pattern could reflect the fact that the *Wab1* phenotype is most severe in the lateral domain. Alternatively, it may be that once correct proximodistal patterning is established within *wab1+/–* tissue, this information can be propagated towards the margins into *Wab1/wab1+* tissue, but only if *Wab1* activity is low. Interestingly, non-autonomy was never documented in *lg1-R;Wab1* plants. Cells in *lg1-R;wab+/–* sectors always had blade identity and cells outside of these sectors always had sheath identity. Thus, *lg1* may affect the autonomy of *Wab1* in both lateral and transverse dimensions.

Mosaic analyses of *lg1-R* have indicated that *lg1* is involved

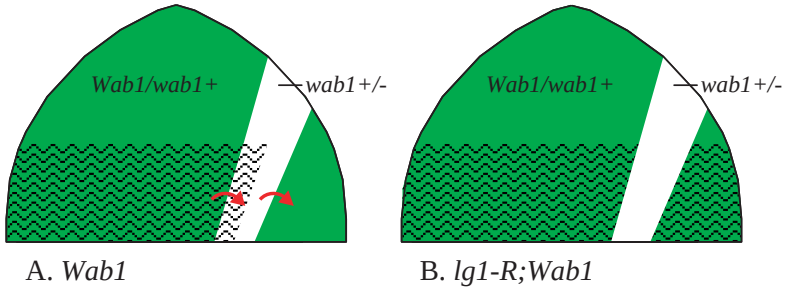

Fig. 6. *lg1* affects cell autonomy of the *Wab1* phenotype. (A) Cartoon illustrating spread of the *Wab1* phenotype (wavy lines) into a *wab1*+/– sector and spread of normal phenotype (no wavy lines) from a sector into *Wab1*/*wab1*+ tissue. We propose that *lg1* may transmit both correct and incorrect positional signals towards the margins of *Wab1* leaves (red arrows). (B) In the absence of *lg1*, the *Wab1* phenotype is strictly cell-autonomous.

in signal propagation, while also acting cell autonomously to induce ligule and auricle (Becraft et al., 1990; Becraft and Freeling, 1991). One of the key findings of this work was the observation that ligule and auricle reinitiated immediately within *Lg1*+/*lg1-R* tissue on the margin side of *lg1-R*/– sectors, but was displaced proximally. The authors interpreted this as evidence that *lg1* is involved in the propagation of a 'make ligule and auricle' signal, and that this signal moves from the midrib towards the margins. Our observations support this hypothesis.

Our data suggest that *Wab1* alters positional information in an autonomous manner, resulting in inappropriate cell differentiation. We speculate that *lg1* is responsible for the non-autonomous effects of *Wab1* that were observed in our mosaic analysis. According to this model, *lg1* may occasionally transmit the signal to initiate ectopic auricle from *Wab1* tissue into *wab1*+/– sectors (Fig. 6A). Similarly, *lg1* may relay correct positioning of the auricle and ligule from *wab1*+/– sectors into adjacent *Wab1* tissue. In the absence of *lg1*, there is no lateral signalling from *Wab1* tissue into *wab1*+/– sectors, or from sectors into *Wab1* tissue (Fig. 6B).

Loss of *Wab1* is associated with an increase in leaf width

We found a significant difference between the widths of sectored (i.e. cells that have lost *Wab1*) and non-sectored leaf-halves in *Wab1* and *lg1-R;Wab1* plants, but not in wild-type or *lg1-R* control plants. No obvious differences in cell width were seen between similar cell types in sectored and non-sectored tissue (data not shown). Therefore, we infer that the increase in lateral growth associated with *wab1*+/– sectors was the result of increased longitudinal cell divisions. It is difficult to determine if increased cell division was confined to the sectored tissue or occurred throughout the sectored leaf-half. The fact that we recorded a significant difference between sectored and non-sectored leaf-half widths suggests that *Wab1* restricts lateral growth with at least some degree of autonomy. If *Wab1* were entirely non autonomous, then the presence of a *wab1*+/– sector would have no effect on leaf-half width. A mosaic analysis of the *tangled* (*tan*) mutation in maize found that the cell division defect is autonomous in both the lateral and transverse dimensions (Walker and Smith, 2002). Thus, there is precedence for strict autonomy of cell division patterns in chimeric tissues.

In both *lg1-R;Wab1* and *Wab1* leaves, sectors positioned near the midrib had no significant effect on leaf-half width, whereas sectors in the outer two thirds of the leaf-half were associated with significant differences between sectored and non-sectored leaf-half widths. This result could reflect the fact that sectors near the midrib tend to be very narrow, and hence have a minimal effect on lateral growth. Alternatively, it may reflect the fact that the *Wab1* phenotype primarily affects regions outside the midrib domain (Hay and Hake, 2004).

The role of *lg1* in leaf morphogenesis

Our study provides evidence of previously unreported functions of *lg1* in leaf morphogenesis. We found that *lg1-R* leaves have longer sheaths and shorter blades than non-mutant (*Lg1*+/*lg1-R*) siblings, thus the blade-sheath boundary is shifted distally (this is shown schematically in Fig. 7A,B). This suggests that *lg1* is required for correct positioning of the blade-sheath boundary.

We also determined that *lg1-R* leaves are narrower at the base of the blade than non-mutant siblings (see Fig. 7A,B). A comparison of clonal sectors in *lg1-R* and wild-type control plants indicates that margin and lateral sectors were significantly narrower in *lg1-R* mutants than in wild-type leaves. These results imply that *lg1* promotes lateral growth at the base of the blade. Sylvester and co-workers (Sylvester et al., 1990) showed that a localised increase in both longitudinal and transverse anticlinal divisions generates a band of small

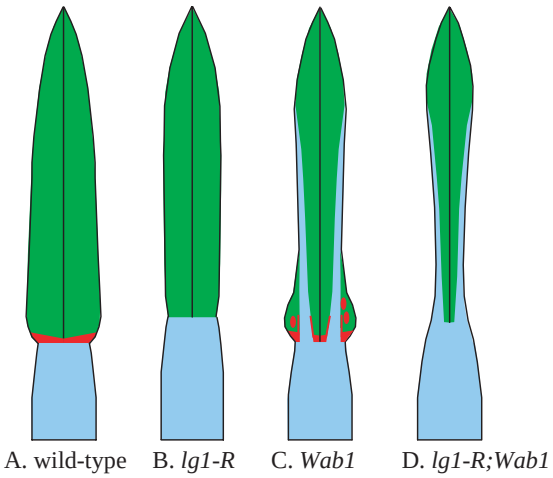

Fig. 7. Model for *lg1* function in leaf morphogenesis. (A) Cartoon of wild-type leaf illustrating distal blade (green) and proximal sheath (blue) separated by ligule and auricle (red). (B) In the absence of *lg1*, ligule and auricle are deleted, the blade-sheath boundary is shifted distally, and the base of the blade is narrower than in wild-type leaves. (C) *Wab1* disrupts proximodistal patterning and restricts lateral growth of the blade. Misexpression of *lg1* in *Wab1* leaves results in ectopic ligule and auricle, and partially compensates for the narrow leaf phenotype at the base of the blade. The lateral signalling function of *lg1* permits some recovery of proximodistal patterning at the margins of *Wab1* leaves. (D) In the absence of *lg1*, *Wab1* leaves never establish blade at the margins and are extremely narrow.

cells across the base of the leaf primordium. This preligule band is a necessary prerequisite for the formation of ligule and auricle. *lg1-R* mutants are specifically defective in longitudinal divisions in the preligule region and at the base of the blade. *lg1* may promote lateral growth via a direct effect on the rate and orientation of cell divisions. Alternatively, the development of the auricle itself may drive lateral growth of the lower leaf blade, ensuring the coordinated expansion of the leaf.

We suggest that the misexpression of *lg1* is responsible for the ectopic auricle and much of the lateral growth at the base of *Wab1* blades. This is reflected in the shape of *Wab1* leaves, which are relatively wide at the base of the blade, but narrow in more distal areas (Fig. 7C). We speculate that the lateral signalling function of *lg1* permits some recovery of proximodistal patterning at the margins of *Wab1* leaves (Fig. 7C). In the absence of *lg1*, *Wab1* leaves never establish blade in this region, and are extremely narrow (Fig. 7D). A cell lineage analysis in *lg1-R*, *Wab1* and double mutant backgrounds, similar to that carried out for *narrow sheath* (Scanlon and Freeling, 1997), would help elucidate cell division patterns in these mutants.

We thank David Hantz for exporting the seed to New Zealand, Ben Parkinson at the Palmerston North Hospital for irradiation of the seeds, Doug Hopcroft and Raymond Bennett for assistance with tissue fixation and plant photography, Alla Seleznyova for help with data analysis, past and present members of the Freeling lab for *lg1-R* material, ideas and information, Jane Langdale, Jennifer Fletcher, Joe Colasanti and our reviewers for helpful comments on the manuscript, and Bruce Veit for tractor driving and stimulating conversations. This work was supported by a Marsden grant from the Royal Society of New Zealand (T.F. and R.J.), a Fulbright scholarship (A.H.) and the United States Department of Agriculture-Agricultural Research Service (S.H.).

References

Becraft, P. and Freeling, M. (1991). Sectors of *liguleless-1* tissue interrupt an inductive signal during maize leaf development. *Plant Cell* **3**, 801-808.

Becraft, P. W., Bongard Pierce, D. K., Sylvester, A. W., Poethig, R. S. and Freeling, M. (1990). The *liguleless-1* gene acts tissue specifically in maize leaf development. *Dev. Biol.* **141**, 220-232.

Bowman, J. L. (2000). The YABBY gene family and abaxial cell fate. *Curr. Opin. Plant Biol.* **3**, 17-22.

Brink, R. A. (1933). Heritable characters in maize XLVI – *liguleless2*. *J. Hered.* **24**, 325-326.

Emerson, R. A. (1912). The inheritance of the ligule and auricles of corn leaves. *Nebraska Agricultural Experimental Station Annual Report* **25**, 81-88.

Esau, K. (1977). *Anatomy of Seed Plants*. New York: John Wiley & Sons.

Foster, T., Yamaguchi, J., Wong, B. C., Veit, B. and Hake, S. (1999). *Gnarley1* is a dominant mutation in the *knox4* homeobox gene affecting cell shape and identity. *Plant Cell* **11**, 1239-1252.

Fowler, J. E. and Freeling, M. (1996). Genetic analysis of mutations that alter cell fates in maize leaves: dominant *Liguleless* mutations. *Dev. Genet*. **18**, 198-222.

Furner, I. J. and Pumfrey, J. E. (1992). Cell fate in the shoot apical meristem of *Arabidopsis thaliana*. *Development* **115**, 755-764.

Harper, L. and Freeling, M. (1996). Interactions of *liguleless1* and *liguleless2* function during ligule induction in maize. *Genetics* **144**, 1871-1882.

Hay, A. and Hake, S. (2004). The dominant mutant *Wavy auricle in blade1* (*Wab1*) disrupts patterning in a lateral domain of the maize leaf. *Plant Phys*. (in press).

Irish, V. F. and Sussex, I. M. (1992). A Fate map of the *Arabidopsis* embryonic shoot apical meristem. *Development* **115**, 745-753.

Kerstetter, R., Bollman, K., Taylor, R. A., Bomblies, K, and Poethig, R. S. (2001). KANADI regulates organ polarity in *Arabidopsis*. *Nature* **411**, 706-709.

Langdale, J. A., Lane, B., Freeling, M. and Nelson, T. (1989). Cell lineage analysis of maize bundle sheath and mesophyll cells. *Dev. Biol.* **133**, 128-139.

Matsumoto, N. and Okada, K. (2003). A homeobox gene, *PRESSED FLOWER*, regulates lateral axis-dependent development of *Arabidopsis* flowers. *Genes Dev.* **15**, 3355-3364.

McConnell, J. R. and Barton, M. K. (1998). Leaf polarity and meristem formation in *Arabidopsis*. *Development* **125**, 2935-2942.

McConnell, J. R., Emery, J, Eshed, Y., Bao, N., Bowman, J. and Barton, K. M. (2001). Role of *PHABULOSA* and *PHAVOLUTA* in determining radial patterning in shoots. *Nature* **411**, 709-712.

Moreno, M. A., Harper, L. C., Krueger, R. W., Dellaporta, S. L. and Freeling, M. (1997). *liguleless1* encodes a nuclear-localized protein required for induction of ligules and auricles during maize leaf organogenesis. *Genes Dev.* **11**, 616-628.

Poethig, R. S. (1984). Cellular parameters of leaf morphogenesis in maize and tobacco. In *Contemporary Problems in Plant Anatomy* (ed. R. A. White and W. C. Dickison). Orlando: Academic Press.

Poethig, R. S. and Szymkowiak, E. J. (1995). Clonal analysis of leaf development in maize. *Maydica* **40**, 67-76.

Russell, S. H. and Evert, R. F. (1985). Leaf vasculature in *Zea Mays*. *L. Planta* **164**, 448-458.

Scanlon, M. J. and Freeling, M. (1997). Clonal sectors reveal that a specific meristematic domain is not utilized in the maize mutant *narrow sheath*. *Dev. Biol.* **182**, 52-66.

Scanlon, M. J., Schneeberger, R. G. and Freeling, M. (1996). The maize mutant *narrow sheath* fails to establish leaf margin identity in a meristematic domain. *Development* **122**, 1683-1691.

Sharman, B. C. (1941). Development of the ligule in *Zea Mays* L. *Nature* **147**, 641.

Sharman, B. C. (1942). Developmental anatomy of the shoot of *Zea mays L*. *Ann. Bot.* **6**, 245-284.

Steffensen, D. M. (1968). A reconstruction of cell development in the shoot apex of maize. *Am. J. Bot.* **55**, 354-369.

Sylvester, A. W., Cande, W. Z. and Freeling, M. (1990). Division and differentiation during normal and *liguleless-1* maize leaf development. *Development* **110**, 985-1000.

Waites, R. and Hudson, A. (1995). *Phantastica*: a gene required for dorsiventrality of leaves in *Antirrhinum majus*. *Development* **121**, 2143-2154.

Walker, K. L. and Smith, L. G. (2002). Investigation of the role of cell-cell interactions in division plane determination during maize leaf development through mosaic analysis of the *tangled* mutation. *Development* **129**, 3219-3226.

Walsh, J., Waters, C. A. and Freeling, M. (1998). The maize gene *liguleless2* encodes a basic leucine zipper protein involved in the establishment of the leaf blade-sheath boundary. *Genes Dev.* **12**, 208-218.